

# **B. TECH. PROJECT REPORT**

On

## **Modelling and Simulation of Hybrid Microgrid**

BY  
**Kishan Narigara**



**DISCIPLINE OF ELECTRICAL ENGINEERING  
INDIAN INSTITUTE OF TECHNOLOGY INDORE  
December 2018**

# Modelling and Simulation of Hybrid Microgrid

**A PROJECT REPORT**

*Submitted in partial fulfillment of the  
requirements for the award of the degrees*

*of*  
**BACHELOR OF TECHNOLOGY**  
*in*

**ELECTRICAL ENGINEERING**

*Submitted by:*  
**Kishan Narigara**

*Guided by:*  
**Dr. Trapti Jain, Associate Professor**



**INDIAN INSTITUTE OF TECHNOLOGY INDORE**  
**December 2018**

### **CANDIDATE’S DECLARATION**

We hereby declare that the project entitled “**Modelling and Simulation of Hybrid Microgrid**” submitted in partial fulfillment for the award of the degree of Bachelor of Technology in ‘Electrical Engineering’ completed under the supervision of **Dr. Trapti Jain, Associate Professor, Electrical Engineering, IIT Indore** is an authentic work.

Further, I/we declare that I/we have not submitted this work for the award of any other degree elsewhere.

**Signature and name of the student(s) with date**

---

### **CERTIFICATE by BTP Guide(s)**

It is certified that the above statement made by the students is correct to the best of my/our knowledge.

**Signature of BTP Guide(s) with dates and their designation**

## **Preface**

This report on “Modelling and Simulation of Hybrid Microgrid” is prepared under the guidance of Dr. Trapti Jain.

Through this report, we have tried to give a detailed modelling of a simple hybrid microgrid with appropriate control and power electronics circuits. The designed microgrid is a combination of photovoltaic (PV) array, MPPT controller, dc-dc boost converter, a common dc bus and an interlinking converter for transferring power from dc to ac sub-grid where ac loads are connected. Modelling and simulations were based on an electromagnetic-transient-analysis program.

We have tried to the best of our abilities and knowledge to explain the content in a lucid manner.

**Kishan Narigara**

B.Tech. IV Year

Discipline of Electrical Engineering

IIT Indore

## **Acknowledgements**

I wish to thank Dr. Trapti Jain for her kind support and valuable guidance.

It is her help and support, due to which I became able to complete the design and technical report.

Without her support, this report would not have been possible.

**Kishan Narigara**

B.Tech. IV Year

Discipline of Electrical Engineering

IIT Indore

## **Abstract**

Hybrid microgrid is emerging as a viable power network for integrating distributed generators and modern dc loads with the existing electrical grid since it combines benefits of both ac and dc systems. This project presents power-control strategies of a hybrid microgrid in grid-connected mode of operation. The microgrid is a combination of photovoltaic (PV) array, MPPT controller, dc-dc boost converter, a common dc bus and an interlinking converter for transferring power from dc to ac sub-grid where ac loads are connected. Microgrid is operated in grid-connected mode to supply load demands uninterruptedly. Interlinking converter efficiently converts dc power generation from PV to ac power and injects into ac bus. Reactive power injection and dc bus voltage are regulated by use of two level control scheme for interlinking converter. The concept and principle of the hybrid microgrid and its control were described. Modeling and simulations were based on an electromagnetic-transient-analysis program. The simulation results were presented to evaluate the dynamic performance of the hybrid system under the grid-connected mode of operation.

## **Table of Contents**

Candidate's Declaration.....	3
Supervisor's Certificate.....	3
Preface.....	4
Acknowledgements.....	5
Abstract.....	6
1) Introduction.....	10
1.1) Introduction.....	10
1.2) Microgrid.....	10
1.3) Microgrid topologies.....	11
1.3.1) AC Microgrid.....	11
1.3.2) DC Microgrid.....	11
1.3.3) AC-DC Hybrid Microgrid.....	12
1.4) Motivation.....	14
2) System Configuration.....	15
2.1) System configuration.....	15
3) Modeling Hybrid Microgrid Components.....	16
3.1) PV array modeling.....	16
3.2) solar I-V and P-V characteristics and MPPT control.....	18

3.3) DC-DC boost converter modeling.....	21
3.4) Interlinking converter modeling.....	21
4) Results and Discussion.....	26
5) Conclusion.....	27
References.....	28
Appendix.....	29

## **List of Figures**

Figure.1: AC-coupled hybrid microgrid or AC microgrid

Figure.2: DC-coupled hybrid microgrid or DC microgrid

Figure.3: AC-DC-coupled hybrid microgrid: structure-I

Figure.4: AC-DC-coupled hybrid microgrid: structure-II

Figure.5: configuration of the hybrid power and control system

Figure.6: Equivalent circuit diagram of a solar cell

Figure.7: solar I-V and P-V characteristics

Figure.8: MPPT control (Incremental Conductance) method

Figure.9: I-V and P-V characteristics of 320 kW PV array

Figure.10: dc-dc boost converter control scheme

Figure.11: VSC as an ILC

Figure.12: ILC control scheme

Figure.13: Active Power Flow diagram

Figure.14: Reactive Power Flow diagram

Figure.15: DC bus voltage (per unit) regulation

Figure.16: Load current (3 phase) during load change at  $t=5.06$  sec

Figure.17: Load current (3 phase) during load change at  $t=9.18$  sec

# Chapter 1

## Introduction

### **1.1** Introduction

The conventional electric grid is an age-old structure planned predominantly for centralized generation of electricity from fossil fuels. Increasing demand and supply shortfall of electricity, peak demand management, need of reducing losses, ageing assets and lack of circuit capacity, fast depletion of fossil fuels and global warming are various other factors affecting the performance of existing grid. Smart grids are being developed as the next generation power systems. These smart grids encompass interconnected microgrids, especially at the distribution level where distributed generations (DGs) are increasingly used. [1] The DG technologies can be classified into power generation from renewable energy (RE) resources such as wind, photovoltaic (PV), micro hydro, biomass, geothermal, ocean wave and tides, the clean alternative energy (AE) generation technologies such as fuel cells (FCs) and micro-turbines, as well as the traditional rotational machine-based technologies such as diesel generators. [1]

### **1.2** Microgrid

Generating and consuming electricity locally is more economical, reliable and efficient, especially for electrification of off-grid or remote communities. This approach has led to a concept of interfacing autonomous and smart electrical network with bidirectional power flow capability popularly referred to as “microgrid”. A microgrid is an aggregation of distributed generation units (DG), distributed energy storage (DES), sensitive and non-sensitive loads, and centralized/decentralized control system, operating as a controllable subsystem, which can operate in grid-connected, as well as in an islanded mode of operation. [2]

## 1.3 Microgrid Topologies

Various microgrid topologies are proposed in literatures. The following section gives an overview of these topologies and their key-features.

### 1.3.1 AC microgrid:

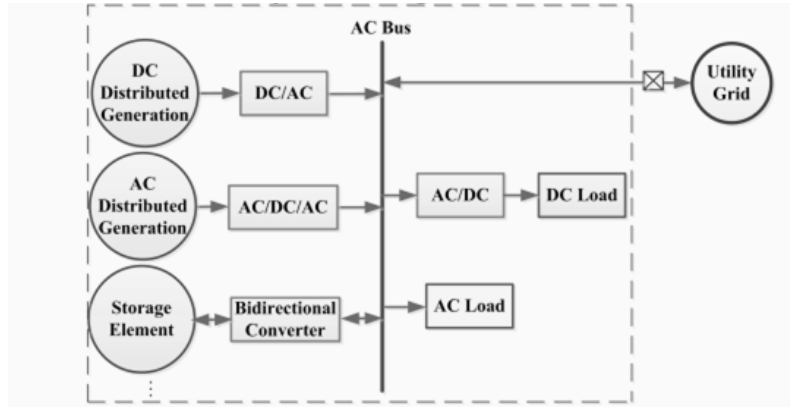


Figure.1: AC-coupled hybrid microgrid or AC microgrid [4]

AC microgrid is proposed to facilitate the interconnection of renewables to conventional power system to reduce generation from fossil fuels, this requires the conversion of many DC sources such as PV and fuel cells to be converted to AC (Hence need of DC-AC conversion). The main bus here (common bus) is AC. The AC microgrid is connected to the utility grid for excess/deficit power sharing and for increasing the reliability of the loads. In case of main grid failure, all the connected DGs and loads need to communicate (exchange power) in the AC platform. Modern Electronic loads work on DC platform, (thus there is a need of AC-DC conversion). In these types of microgrid, DC-AC-DC conversion stages are more common.

### 1.3.2 DC microgrid:

The recent surge in the concept of DC microgrid facilitates direct connection of renewables like PV, fuel cell and DC loads. The main bus here (common bus) is DC. The DC microgrid is connected to the utility grid for excess/deficit power sharing and for increasing the reliability of the loads. In case of main grid failure, all the connected DGs and loads need to communicate (exchange power) in the DC platform. However, the DC microgrid alone does not

allow direct interconnection of renewables like wind (Require AC-DC conversion). In addition, industrial and motor loads cannot be directly fed through DC grid (DC-AC connection is mandatory).

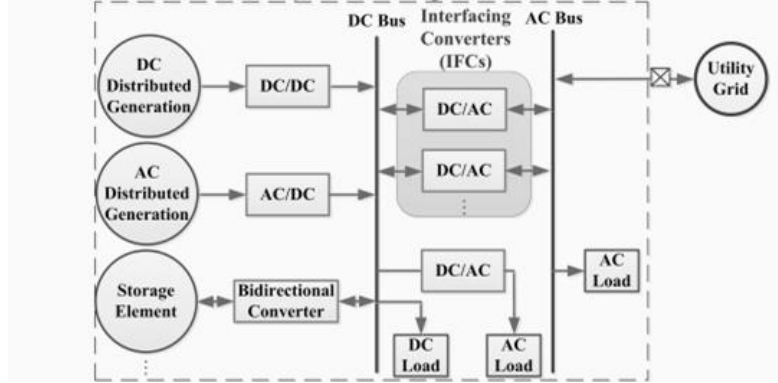


Figure.2: DC-coupled hybrid microgrid or DC microgrid [4]

### 1.3.3 AC-DC hybrid microgrid:

The main bus here (common bus) is both AC and DC. The hybrid microgrid is connected to the utility grid for excess/deficit power sharing and for increasing the reliability of the loads. In case of main grid failure, all the connected DGs and loads can communicate in both AC and DC platform. It is a combination of AC and DC microgrid to be named as hybrid microgrid. Both AC and DC microgrid contains DGs, loads and may be storage system. Both the microgrid are connected together through single/multiple AC-DC inverter that helps to transfer excess/deficit power from one microgrid to another. The main control objectives of AC/DC hybrid microgrid is to achieve power balance within the individual microgrid most of the time.

#### 1.3.3.1 Structure-I

Both DC and AC buses have DGs and SEs, and these buses are linked by Inter linking Converters (ILCs). The AC–DC coupled hybrid microgrid has distributed generations (DGs) and Storages (SEs) on both AC and DC buses. There is a need of robust coordination between the DC and AC subsystems for the voltage and power control. In general, this structure is considered if major power sources include both DC and AC powers. However, DC–AC–DC or AC–DC–AC conversions are inevitable in this type of structures as both DC/AC sources and loads are connected to both the buses.

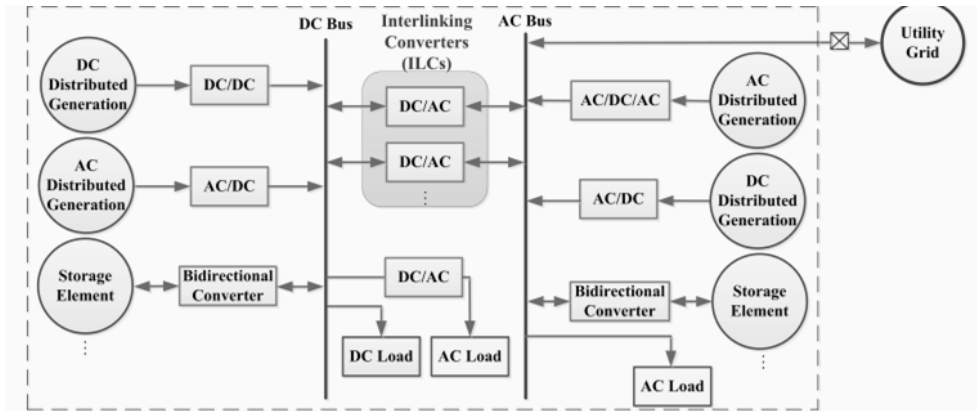


Figure.3: AC-DC-coupled hybrid microgrid: structure-I [4]

### 1.3.3.2 Structure-II

Mainly AC sources and loads are connected to the AC network whereas DC sources and loads are tied to the DC network. This structure has the key benefit that the processes of multiple DC–AC–DC or AC–DC–AC conversions reduces significantly in an individual AC or DC grid. This structure improves overall efficiency and reduces the system cost with reduced number of power converters by connecting sources and loads to the AC and DC buses with minimized power conversion requirements.

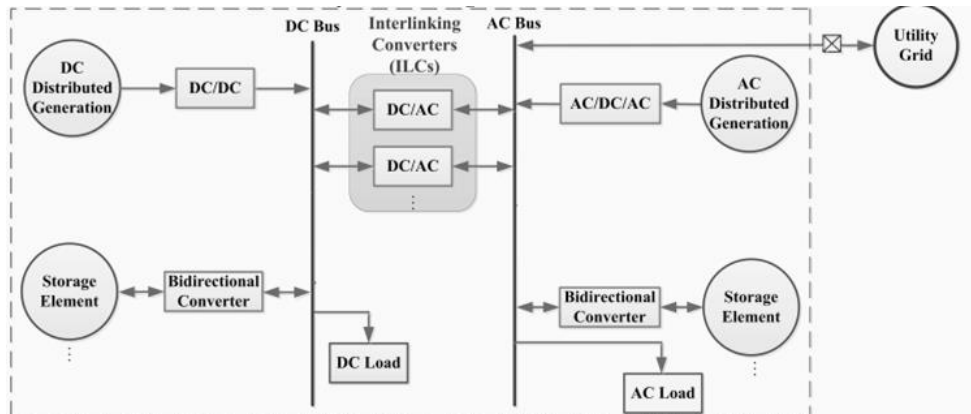


Figure.4: AC-DC-coupled hybrid microgrid: structure-II

## **1.4 Motivation**

Accurate modelling of the system is of utmost importance for developing and testing control strategies. Power management strategies proposed for hybrid microgrid till now have usually used aggregated models for the ac and dc sub-grids. However, these aggregated models are not useful for studying aspects such as power quality at various points inside the sub-grids, power scheduling/dispatch, distribution network planning, etc., for which detailed modelling of subsystems is needed. [4] Continued research efforts are still needed to develop and test complete and accurate models of various subsystems and of hybrid microgrid as a whole. This work intends to model a simple hybrid AC/DC microgrid architecture and simulate the same in an electromagnetic transient simulator program.

# Chapter 2

## System Configuration

### 2.1 System configuration

Figure.5 presents the configuration of the hybrid power and control system. The microgrid consists of a PV array with dc-dc boost converter, a common dc bus, interlinking converter, a common ac bus, variable ac loads and connection main grid (distribution network). The PV system consists of a PV array and a step-up dc-dc converter for boosting the array voltage to a higher level of common dc voltage. The dc-ac interlinking inverter transfers into AC sub-grid dc-power generation from the PV array in the form of ac power. The control system of the hybrid generation is a distributed control. Local controllers include a PV array controller and an interlinking converter controller, which are all built in a hybrid power conditioning system. Variable ac loads are connected to common ac bus through circuit breakers. AC sub-grid is connected to main grid for grid-connected mode of operation.

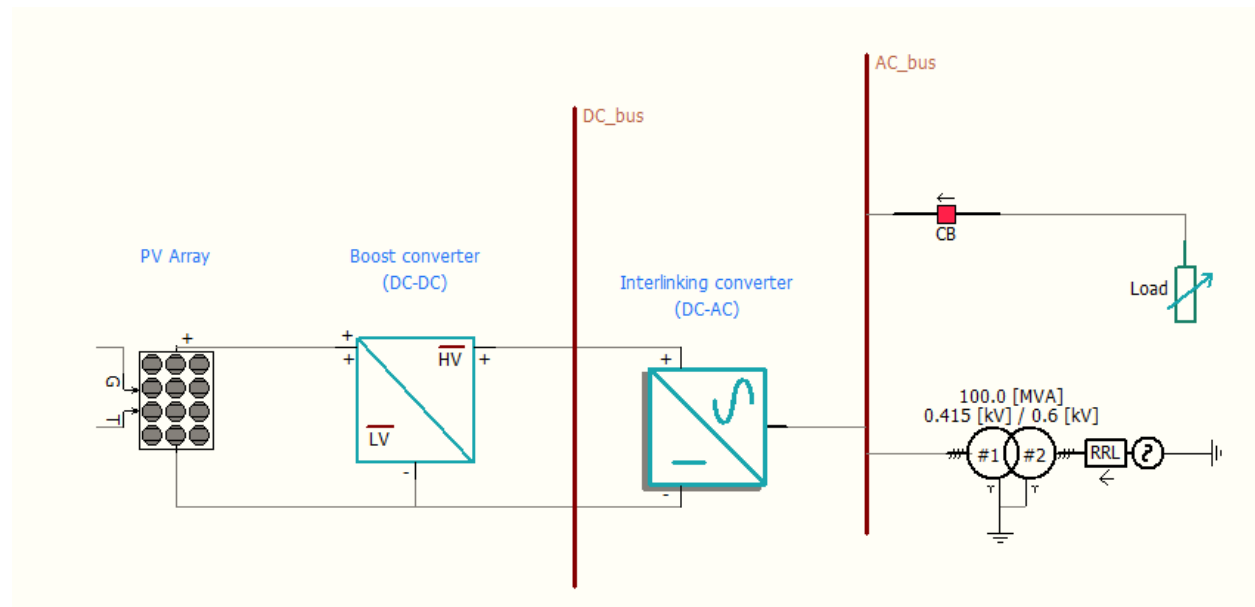


Figure.5: configuration of the hybrid power and control system

## Chapter 3

### Modelling of hybrid microgrid components

#### 3.1 PV array modeling

The detailed modelling of a PV array is presented in this section. Figure.6 shows an equivalent circuit diagram of a single solar cell.

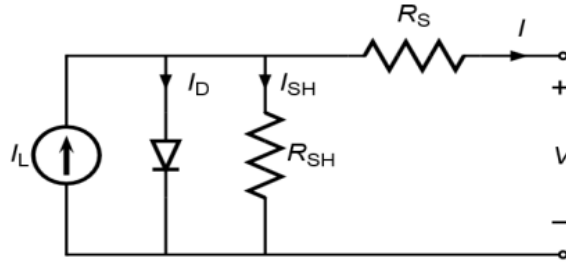


Figure.6: Equivalent circuit diagram of a solar cell

Significant power losses caused by the presence of a shunt resistance,  $R_{SH}$ , are typically due to manufacturing defects, rather than poor solar cell design. Series resistance in a solar cell has three causes: (i) the movement of current through the emitter and base of the solar cell, (ii) the contact resistance between the metal contact and the silicon, (iii) the resistance of the top and rear metal contacts. The main impact of series resistance  $R_S$  is to reduce the fill factor, although excessively high values may also reduce the short-circuit current. Equations (1) to (3) represents cell output current, light-generated current and diode reverse saturation current respectively. [6]

$$I = I_L - I_0 e^{\frac{q(V+IR_S)}{\eta k T_C}} - \frac{V + IR_S}{R_{SH}} \quad \dots \dots \dots (1)$$

$$I_L = I_{SC,r} [1 + \alpha_{SC} (T_C - 28^\circ)] \times \frac{G_C}{G_r} \quad \dots \dots \dots (2)$$

$$I_0 = I_{0r} \left( \frac{T_C}{T_r} \right)^3 e^{\left[ \frac{q E_g}{\eta k} \left( \frac{1}{T_C} - \frac{1}{T_r} \right) \right]} \quad \dots \dots \dots (3)$$

Where  $k$  = Boltzmann constant =  $1.38 \times 10^{-23}$  J/K,

$q$  = electronic charge =  $1.6 \times 10^{-19}$  C,

$\eta$  = ideality factor,

$E_g$  = band-gap energy (eV),

$T_C$  = cell temperature,

$T_r$  = reference temperature =  $28^\circ$  C,

$I_{SC,r}$  = short-circuit current at reference temperature,

$I_{0r}$  = reverse saturation current at  $T_r$ ,

$\alpha_{SC}$  = short-circuit current temperature coefficient,

$G_C$  = cell illumination ( $W/m^2$ ),

$G_r$  = reference cell illumination ( $W/m^2$ ).

Since PV arrays are built up with series and/or parallel connected combinations of solar PV cells, for an array with  $n_s \times n_p$  cells, the current equation can be presented as

$$I_{PV} = n_p I_L - n_p I_0 \left[ \exp \left( \frac{q}{\eta k T_C} \left( \frac{V_{PV} + I_{PV} R_S}{n_s} \right) \right) - 1 \right] - \frac{V_{PV} + I_{PV} R_S}{R_{SH}} \quad \dots \dots \dots (4)$$

Where  $I_{PV} = n_p \times I_{cell}$  = PV array output current,

$V_{PV} = n_s \times I_{cell}$  = PV array output voltage,

$n_s$  = number of cells in series,

$n_p$  = number of panels in parallel,

$R_S = R_{S,cell} \times \frac{n_s}{n_p}$  = PV array series resistance,

$R_{Sh} = R_{Sh,cell} \times \frac{n_s}{n_p}$  = PV array shunt resistance.

Using all the above equations, a 320 kW PV array was modelled with parameters as listed in table 1.

Number of modules connected in series per array	22
Number of module strings in parallel per array	250
Number of cells connected in series per module	36
Number of cells connected in parallel per module	1
Reference irradiation	1000 W/m <sup>2</sup>
Reference cell temperature	28 °C
Effective area per cell	0.01 m <sup>2</sup>
Series resistance per cell	0.02 ohm
Shunt resistance per cell	1000 ohm
Diode ideality factor	1.5
Band gap energy	1.013 eV
Saturation current at reference condition per cell	1×10 <sup>-9</sup> A
Short circuit current at reference condition per cell	2.5072 A
Temperature coefficient of photo current	0.001 A/°C

Table.1: PV array parameters

### **3.2 Solar I-V and P-V characteristics and MPPT control**

The characteristics of a solar cell is affected by solar irradiance and temperature as shown in fig.7. The power characteristics of a PV module can be derived from I-V characteristics. The power increases until it reaches optimal voltage ( $V_{mp}$ ) at the knee point of the curve. Above the  $V_{mp}$ , PV output decreases until it reaches zero at open-circuit voltage. Below  $V_{mp}$ , PV behavior is similar to a current source and above  $V_{mp}$ , PV behavior is similar to a voltage source.

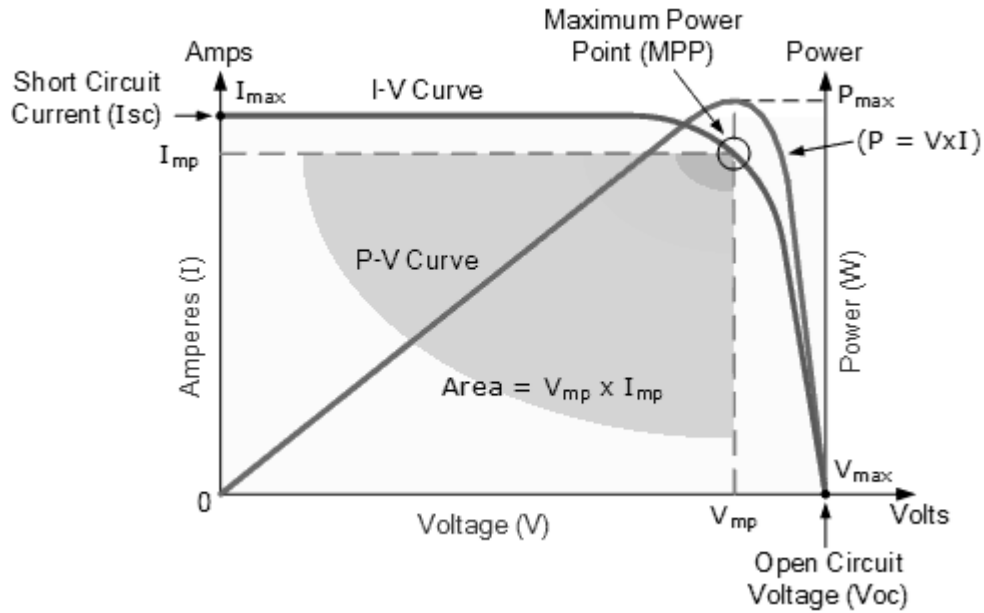


Figure.7: solar I-V and P-V characteristics [6]

Power output of a PV array depends on the voltage level where it operates under a given condition of irradiance and cell-surface temperature. For efficient operation, a PV array should operate near at the peak point of the  $V$ - $P$  curve.

Researchers have proposed various MPPT techniques such as Perturb & Observe, Incremental Conductance, Hill Climbing method, etc. for maximum power point tracking. The incremental conductance method (fig.8) was implemented in this project. The MPPT block senses the PV array current  $i_{PV}$  and array voltage  $V_{PV}$  and returns the array voltage command.

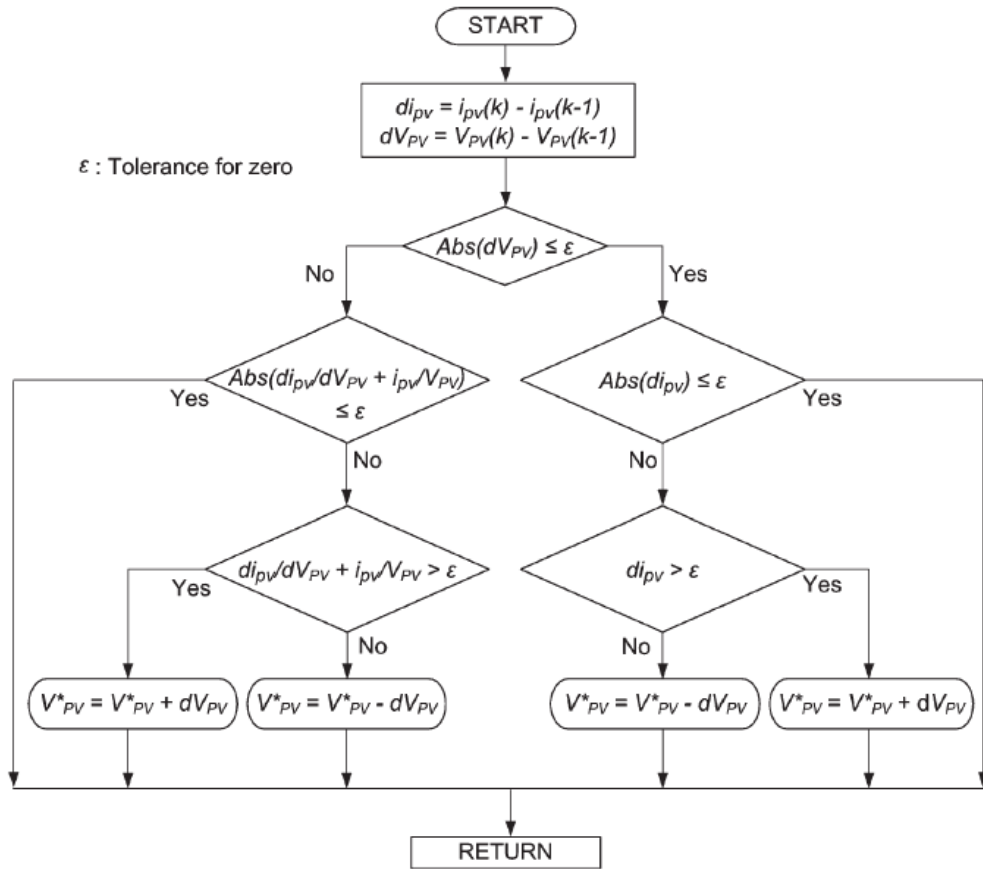


Figure.8: MPPT control (Incremental Conductance) method

When applied for the modelled PV array following results were obtained.

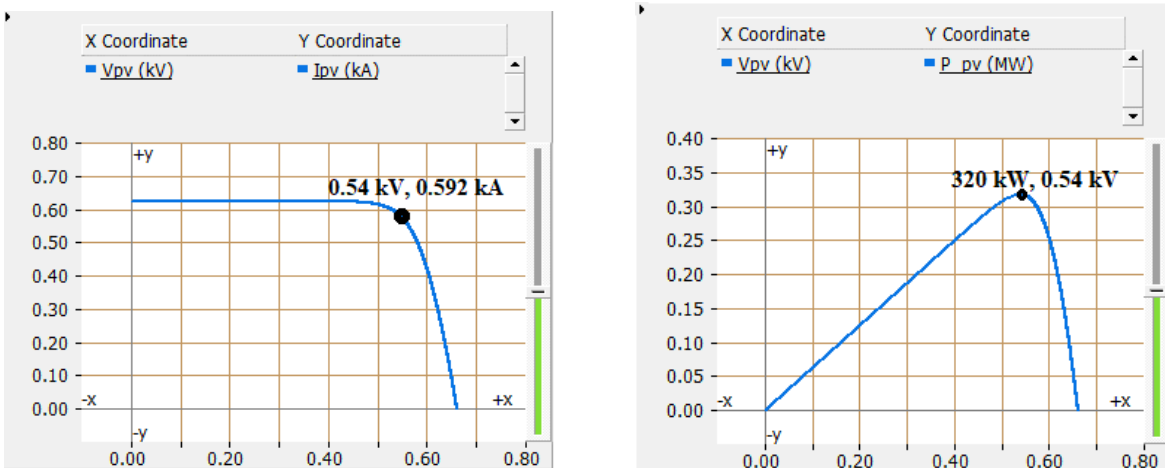


Figure.9: I-V and P-V characteristics of 320 kW PV array

### 3.3 DC-DC boost converter modeling

Following the MPPT controller, a dc-dc boost converter is used to step up the PV array output voltage  $V_{PV}$  to common DC bus voltage  $V_{DC}$ . The control scheme for this converter is as shown in the fig.10.

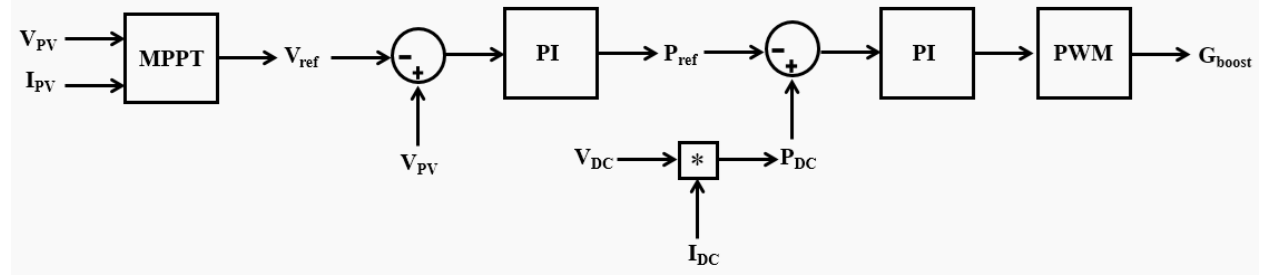


Figure.10: dc-dc boost converter control scheme

The converter regulates the array voltage  $V_{PV}$  at the reference voltage  $V_{ref}$  commanded by the maximum power point tracking (MPPT) controller and boosts it to the level of common dc voltage. Error between the ordered and real voltage is processed through the voltage controller into the ordered power  $P_{ref}$ , which is compared with the output power  $P_{DC}$  at converter output terminal (that is common dc bus). Error between ordered and actual power at converter output terminals is processed through power controller into modulating signal for PWM that then outputs gate signal  $G_{boost}$  for the converter.

### 3.4 Interlinking converter modeling

The Interlinking converter (ILC) can act as a rectifier or an inverter depending on the direction of power flow needed at each instant. It typically controls the dc bus voltage when the hybrid microgrid is connected to the grid. Different converter topologies and configurations can act as interlinking converter to facilitate power exchange among dc/ac sub-grids and the main grid. The most suitable single-stage interlinking converter for conventional hybrid microgrid topology is a pulse width modulated (PWM) bidirectional voltage source converter (VSC) as shown in Fig. 11. [4]

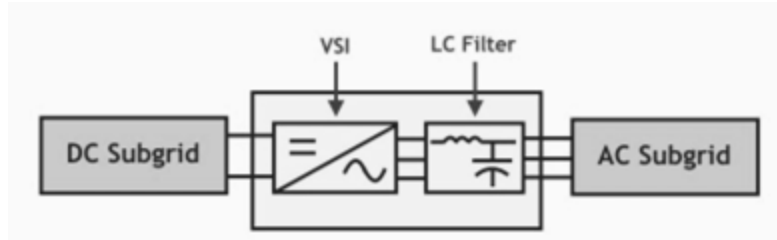


Figure.11: VSC as an ILC [4]

VSC can be controlled in voltage controlled mode (VCM) to regulate the ac or dc bus voltage or it can operate in current controlled mode (CCM) to regulate the power flow. In grid-connected mode, ILC is generally responsible for maintaining the dc bus voltage. Reactive power flow is not a major concern for the ILC since it is demanded only by the ac sub-grid. [4] The ILC should contribute to the reactive power demand only when the active power flow is from dc to ac side whereas the reactive power set point should be set to zero when the active power flow is from ac to dc side.

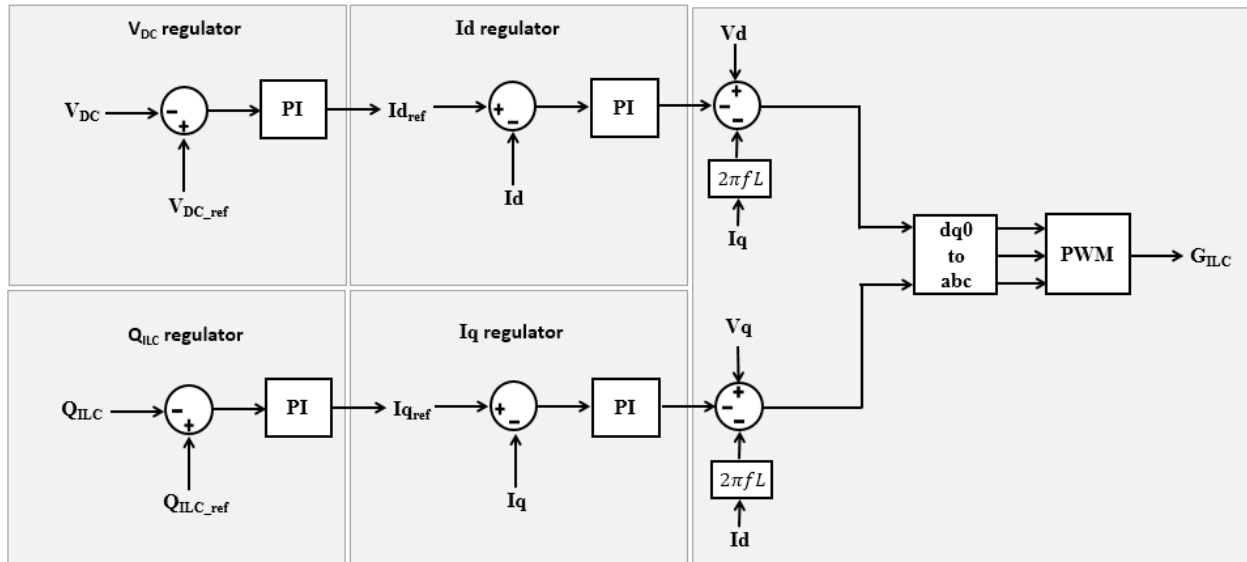


Figure.12: ILC control scheme

The ILC controller consists of a reactive power controller, dc bus voltage controller and a d-q-frame-based current controller as shown in fig.12. The upper level controller regulates the dc bus voltage and reactive power flow,  $V_{DC}$  and  $Q_{ILC}$ , and outputs the d- and q-axis current commands  $I_{qref}$  and  $I_{dref}$  at which the lower level current controller regulates the d-q components of ac current. Outputs of these lower level controllers are then processed to generator gate signal  $G_{ILC}$  for ILC.

## Chapter 4

### Results and Discussion

#### 4.1 Simulation results

Grid-connected solar PV system has two parallel power supplies, one from the solar PV system and the other from the power grid. The combined power supply feeds all the loads connected to the AC bus. Whenever the solar PV supply exceeds the load demand, excess electricity will be exported into the grid. When the PV generation is less than the load demand, the power grid will supply deficit power to the load.

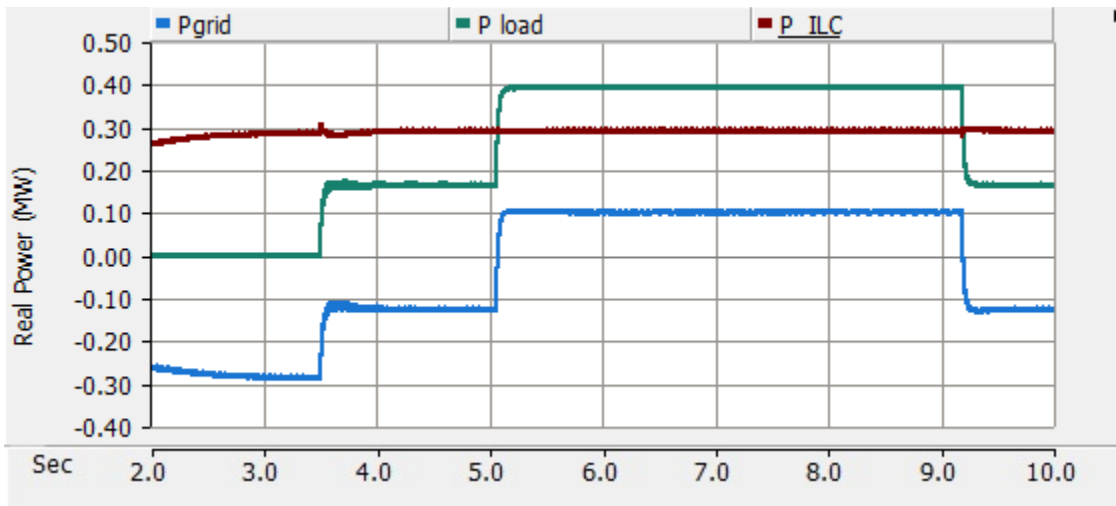


Figure.13: Active Power Flow diagram

P\_ILC is the power transferred from dc to ac sub-grid that is 300 kW constant power generated from PV source on the DC sub-grid. P\_grid shows the net power injected into ac bus of the hybrid microgrid. Loads connected to AC sub-grid are switched on at different times as shown in above fig.13. Before  $t=3.5$  sec, all of the PV generation is fed to the main grid. A load of 170 kW (+85 kVAr) is switched on at  $t=3.5$  sec that is then supplied by ILC and remaining power (100 kW) is exported to main grid. At  $t=5.06$  sec another load of 230 kW is switched on,

since maximum power delivered to ac grid by ILC is 300 kW, shortfall of supply is balanced by main grid that injects power to ac bus. This load is again switched off at  $t=9.18$  sec as shown in power diagrams.

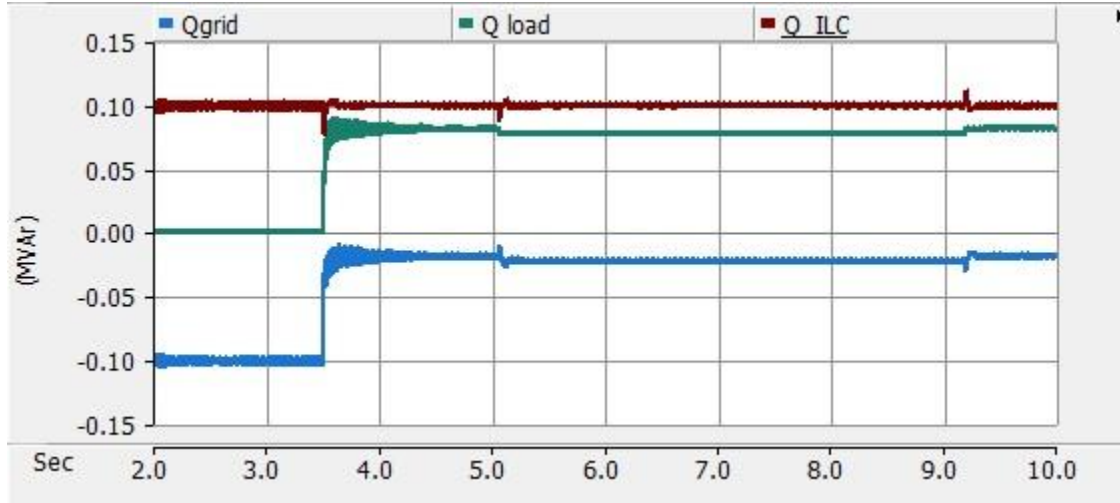


Figure.14: Reactive Power Flow diagram

$Q_{ILC}$  is regulated to  $Q_{ILC,ref}$  ( $=10$  kVAR) in this simulation by control loop of ILC as explained in the previous chapter. This reactive power is fed to main grid before  $t=3.5$  sec and partially (85 kVAR) delivered to load after  $t=3.5$  sec.

DC bus voltage is also regulated by ILC in specified limits during different loading conditions as shown in fig.15.

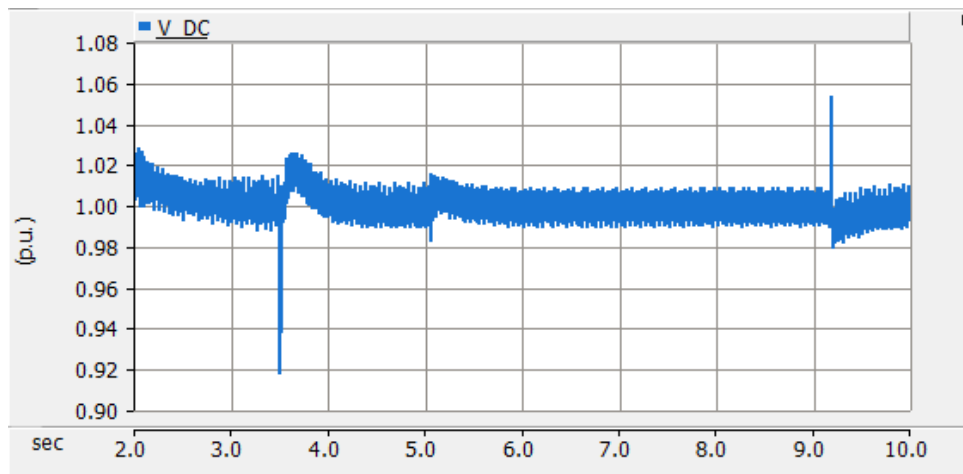


Figure.15: DC bus voltage (per unit)

Load currents during these different loading conditions were as shown in fig.16 and fig.17.

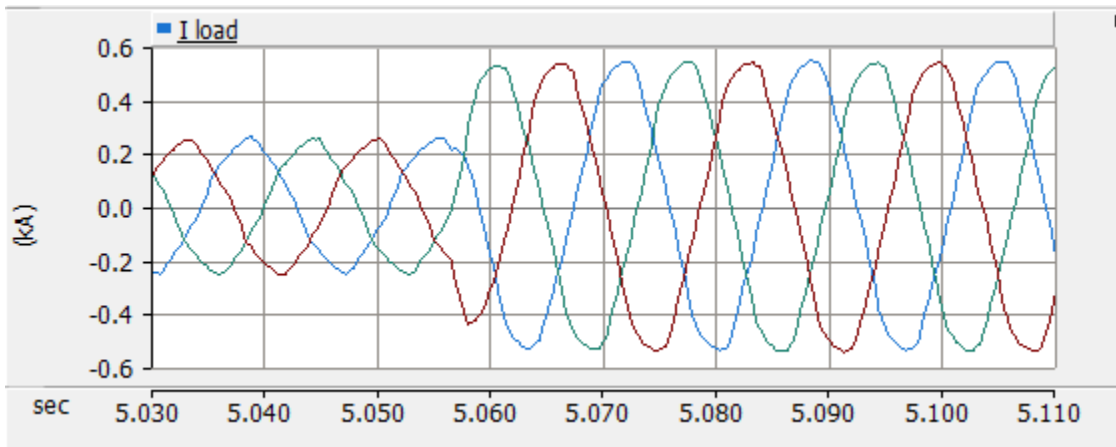


Figure.16: Load current (3 phase) during load change at  $t=5.06$  sec

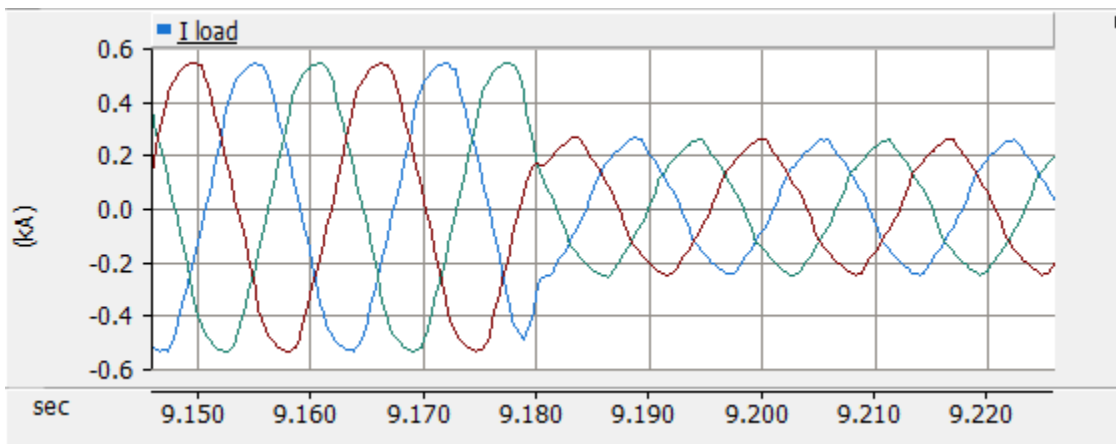


Figure.17: Load current (3 phase) during load change at  $t=9.18$  sec

# **Chapter 5**

## **Conclusion**

- 1) A 320 kW PV array with MPPT implementation for harnessing maximum power from PV was modelled and simulation results were in accordance with theoretical values.
- 2) A DC-DC boost converter for integrating PV to common DC bus was modelled with PI controllers and voltage control loops for converting PV output voltage to common DC bus voltage.
- 3) A VSC with two levels of control was used as an interlinking converter to transfer power from dc grid to ac grid efficiently.
- 4) Interlinking converter control limited DC bus voltage fluctuations within  $\pm 5\%$ . It also regulated the reactive power flow from dc to ac sub-grid.
- 5) In grid connected mode, simulation results show that load demand is mostly balanced by instantaneous PV generation whereas shortfall of supply is balanced by main grid. Use of storage systems should be investigated to reduce dependency on distribution grid.

## References

- [1] F. Nejabatkah and Y. W. Li, "Overview of Power Management Strategies of Hybrid AC/DC Microgrid," in IEEE Transactions on Power Electronics, vol. 30, no. 12, pp. 7072-7089, Dec. 2015.
- [2] S. K. Sahoo, A. K. Sinha and N. K. Kishore, "Control Techniques in AC, DC, and Hybrid AC-DC Microgrid: A Review," in IEEE Journal of Emerging and Selected Topics in Power Electronics, vol. 6, no. 2, pp. 738–759, Jun. 2018.
- [3] E S N Raju P and Trapti Jain, "Hybrid AC/DC Micro Grid: An Overview," Fifth International Conference on Power and Energy Systems, Oct. 2013.
- [4] A. Gupta, S. Doolla, K. Chatterjee, "Hybrid ac-dc microgrid: Systematic evaluation of control strategies", IEEE Transactions on Smart Grid, vol. 9, no. 4, pp. 3830-3843, July 2018.
- [5] J. Zhang, D. Guo, F. Wang, Y. Zuo, and H. Zhang, "Control strategy of interlinking converter in hybrid AC/DC microgrid," in Renewable Energy Research and Applications (ICRERA), 2013 International Conference on, Oct 2013, pp. 97–102.
- [6] <https://nptel.ac.in/courses/108107113/7>
- [7] J.M. Guerrero, M. Chandorkar, T. Lee, P.C. Loh, "Advanced control architectures for intelligent microgrids – part I: decentralized and hierarchical control", IEEE Trans. Ind. Electron., vol. 60, no. 4, pp. 1254–1262, April 2013.

## Appendix

### Parameter values used in simulations:

#### 1) Power topology of hybrid microgrid (refer fig.5)

Power Topology		
AC grid	bus voltage (L-L rms)	415 V
	frequency	60 Hz
DC grid	bus voltage	700 V

#### 2) DC-DC boost converter parameters (refer fig.10)

DC-DC boost converter		
Voltage outer loop (PI)	$K_p$	1
	$K_i$	0.05
Power inner loop (PI)	$K_p$	1
	$K_i$	0.5
PWM	Switching frequency	5 kHz

3) DC-AC interlinking converter parameters (refer fig.11,12)

DC-AC interlinking converter		
V <sub>DC</sub> regulator (PI)	<i>Kp</i>	0.5
	<i>Ki</i>	0.2
Q <sub>ILC</sub> regulator (PI)	<i>Kp</i>	0.3
	<i>Ki</i>	0.02
Id regulator (PI)	<i>Kp</i>	0.15
	<i>Ki</i>	0.08
Iq regulator (PI)	<i>Kp</i>	0.15
	<i>Ki</i>	0.08
PWM	<i>Switching frequency</i>	8 kHz
LC filter	<i>L (uH)</i>	300
	<i>C (uF)</i>	200